한국현미경학회지 제39권 제4호 2009
Korean J. Microscopy 39(4), 291~299(2009)

Populations of Rod and Cone Photoreceptors in the Hamster Retina

Song-Hee Yu*, Hyun-Jin Kim, Kyoung-Pil Lee, Eun-Shil Lee, Jea-Young Lee and Chang-Jin Jeon

Department of Biology, College of Natural Sciences, and Brain Science and Engineering Institute, Kyungpook National University, Daegu 702-701, Korea
(Received September 23, 2009; Accepted December 24, 2009)

햄스터 망막에서의 광수용체 분포

유성희*, 김현진, 이경필, 이은실, 이제영, 전창진

경북대학교 자연과학대학 생물학과, 생명과학 및 뇌 과학 연구소

ABSTRACT

We report on a quantitative analysis of cone and rod photoreceptors in hamster retina. Cone and rod photoreceptors were counted in retinal whole mounts using differential interference contrast (DIC) optics microscopy after staining of cone photoreceptors were stained with peroxidase-labeled peanut lectin. Middle-to-long-wave-sensitive-(M/L-), and short-wave-sensitive-(S-) cone opsins were visualized by observed using confocal microscope after immunocytochemical procedure. The average cone density was 9,307 cells/mm^2, giving a total of cones of 293,060 cone cells per retina. The peak density of cone cells (12,857 cells/mm^2) was found 0.3 mm from the optic disk (OD) of the nasal retina. The average rod density was 300,082 cells/mm^2, giving a total number of rods of 9,448,150 cells. The peak density of rod cells was found 0.3 mm from the OD of the dorsal retina. Of all photoreceptors studied, the total percentage of rods and cones were 96.99% and cones 3.01%, respectively. The mean ratio of rod and cone was 32.24 : 1. The cone photoreceptors of hamster contained both M/L- and S-cone opsins. The present results suggest that the hamster retina is strongly rod-dominated with some photopic property of vision.

Keywords : Cones, Density, Photoreceptors, Retinal mosaic, Rods

INTRODUCTION

Most vertebrate retina have scotopic and photopic visual systems. The rod-dependent scotopic visual system mediates vision in dim light, and the cone-dependent photopic visual system mediates vision in bright light (Wikler & Rakic, 1990; Rodieck, 1998). In many animals, cone photoreceptors are also essential for color vision. Since the differences in the spatial density and distribution of the photoreceptors within the retina are the most fundamental determinants of visual processing information, the basic organization of the photoreceptor mosaic has been well characterized in several animals. For example, Packer et al. (1990) and Wikler et al. (1990) identified the photoreceptor topography in monkey retina. Curcio et al. (1990) and Chandler et al. (1999) identified photoreceptor

This Research was supported by Kyungpook National University Research Fund, 2008.
* Correspondence should be addressed to Prof. Chang-Jin Jeon, Neuroscience Laboratory, Department of Biology, College of Natural Sciences, Kyungpook National University, 1370 Sankyuk-dong, Daegu 702-701, Korea. Ph.: (053) 950-5343, Fax: (053) 953-3066, E-mail: cjjeon@knu.ac.kr

topography in human and pig, respectively. The density of cone and rod photoreceptors in ground squirrel and mouse has been identified by Kryger et al. (1998) and our group (Jeon et al., 1998) respectively. Recently, the cone and rod photoreceptor populations in the retina of the bat have also been reported by our group (Kim et al., 2008).

Hamster has been used in a broad range of biomedical studies. It is, however, surprising that no study of the number and density of both rods and cones in hamster retina has been carried out. Thus, our goal was to investigate the population of both rods and cones in hamster retina. As vision is an important sense in most mammals, this goal will provide critical requirements in understanding the cellular architecture of the hamster retina and the quality of visual information processing in the hamster retina.

MATERIALS AND METHODS

1. Animals and tissue preparation

Adult Syrian hamsters (*Mesocricetus auratus*) (20～30 g) were used in this study. Animals were anesthetized with a mixture of ketamine hydrochloride (30～40 mg/kg) and xylazine (3～6 mg/kg). A local anesthetic, proparacaine hydrochloride (100～200 μL), was applied to the cornea to suppress blink reflexes. The eyes were enucleated after a reference point was taken to label the superior pole, and were immediately immersed in 4% paraformaldehyde in 0.1 M phosphate buffer (PB, pH 7.4). The anterior segments of the eyes were removed and the retinas were isolated from the eyecup and post-fixed for 2 hr in 2.5% glutaraldehyde in 0.1 M PB. After being rinsed 3× 10 min in 0.1 M PB, retina tissues were processed as whole mounts. Retinal tissues were processed as whole mounts and were cut vertically into 50 μm thick sections using a vibratome. The guidelines of the National Institute of Health regarding the Care and Use of Laboratory Animals were followed in all experimental procedures.

2. Total cone photoreceptor staining

The whole mount retinas were incubated in 50 μg/mL peroxidase-labeled peanut lectin (PNA, Sigma, St. Louis, MO, USA) in 0.25 M Tris buffer, for 16～18 hr (Bridges, 1981; Blanks et al., 1984; Jeon et al., 1998). PNA is known as a general marker for labeling cone cells. Labeled cells were visualized using a diaminobenzidine (DAB) reagent kit (Kirkegaard & Perry, Gaithersburg, MD, USA) in 0.25 M Tris buffer. Retinas were then rinsed, mounted flat on Superfrost Plus slides (Fisher, Pittsburgh, PA, USA), and coverslipped with DMSO. After 12 hr, DMSO was replaced with 100% glycerol.

3. Immunocytochemistry for cone opsins

A polyclonal antibody against middle-to-long-wave-sensitive- (M/L-) opsin was obtained from Chemicon (Temecula, CA, USA). A polyclonal antibody against short-wave-sensitive- (S-) opsin was obtained from Santa Cruz (Santa Cruz, CA, USA). These two antibodies have been widely used to label M/L-opsin and S-opsin respectively. The primary antiserum was diluted by the ratio of 1 : 250 (M/L-opsin and S-opsin). Standard immunocytochemistrical methods have been described in detail in our previous studies (Jeon & Jeon, 1998; Jeon et al., 1998). For detection by immunofluorescence, the secondary antibody was fluorescein (FITC) conjugated anti-rabbit IgG (Vector Lab., Burlingames, CA, USA) for detecting the anti-M/L-opsin and anti-S-opsin. Labeled sections were coverslipped with Vectashield mounting medium (Vector Lab.). Images were obtained on a Bio-Rad MRC 1024 laser scanning confocal microscope.

4. Quantitative analysis of cones and rods

Both labeled cones and unlabeled rods could be examined and photographed on a Zeiss Axioplan microscope using high power differential interference contrast (DIC) optics (Curcio et al., 1987; Jeon et al., 1998). Cell density was expressed as the number of PNA-labeled cells/mm^2 of retinal surface. In three DAB-reacted whole mount retinas, PNA-labeled cone cells were viewed on a computer monitor using a Zeiss Plan-Apochromat 100× objective and a Zeiss AxioCam HRc digital camera at 300 μm intervals along the central dorsoventral and nasotemporal axes. The sample areas for counting the cone cells were 70×70 μm^2. A transparency sheet was placed on the computer monitor, and labeled cells were circled with a pen. The samples were taken only at well-labeled positions across the retinas. In three DAB-reacted whole mount retinas, unlabeled rod cells were viewed on a computer monitor using the same objective and digital camera at 300 μm intervals along the central dorsoventral and nasotemporal axes. The sample areas for counting the rod cells were 30×30 μm^2. The total number of cells was determined in each sample area and expressed as the number of cells/mm^2. The cell density was multiplied by retinal area to determine the total number of cells.

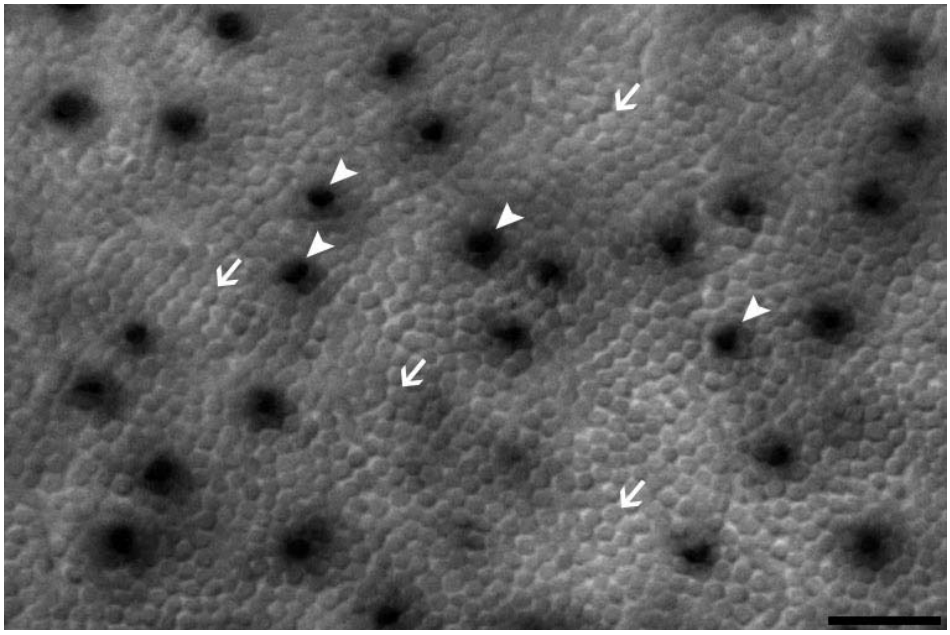

Fig. 1. High magnification differential interference micrographs of cone and rod photoreceptors in a whole mount tissue in hamster retina. The lighter cells are rod inner segments and the darker cells are cone inner segments by the diaminobenzidine reaction product. Arrows indicate some rod cells, and arrowheads indicate some cone cells. Scale bar=10 μm.

Table 1. The densities of photoreceptor in Syrian hamster

Retina	Sampled area (n)	Sampled area (μm^2)[a]	Cone cells counter	Total retinal area (mm^2)	Mean density (cells/mm^2)	Total cone cells
Retina 1L	40	196,000	1,807	31	9,219	290,226
Retina 2L	39	191,100	1,819	31	9,519	295,076
Retina 3R	40	196,000	1,800	32	9,184	293,878
Mean±SD					9,307±184	293,060±2,526

Retina	Sampled area (n)	Sampled area (μm^2)[b]	Rod cells counter	Total retinal area (mm^2)	Mean density (cells/mm^2)	Total rod cells
Retina 1L	44	39,600	12,118	31	306,010	9,633,198
Retina 2L	42	37,800	11,503	31	304,312	9,433,677
Retina 3R	44	39,600	11,481	32	289,924	9,277,576
Mean±SD					300,082±8,838	9,448,150±178,252

L, left; R, right

[a]One sampled area=70×70 μm^2; [b]One sampled area=30×30 μm^2

RESULTS

Fig. 1 shows mosaic of cones and rods in peripheral region of the hamster retina. PNA-labeled cones (outlined darkly, arrowhead) as well as unlabeled rods (outlined lightly and more or less polygonal in shape, arrow) could be observed in this high power DIC picture.

In three DAB-reacted whole mount retinas, cone cells in the photoreceptor cell layer were counted. The estimated total number of cone cells varied from 290,226 to 295,076 cells among the three sampled retinas in this study. Table 1 and Fig. 2 show the results. There were 290,226 cells in retina #1L, 295,076 cells in retina #2L, and 293,878 cells in retina #3R; therefore, the average number of cone cells/retina was 293,060±2,526 (mean±SD; n=3). The mean density of cone cells was 9,307 ±184 cells/mm^2 in the three retinas (Table 1). The distribution of total cone cells is shown in Fig. 2 and Table 2. The two graphs (Fig. 2a and 2b) show the numbers of cells encountered along the nasotemporal (Fig. 2a) and dorsoventral (Fig. 2b) axes intersecting the optic nerve head (OD). In the present study, the lowest density of cone cells (4,694±577, mean±SD; n=3) was found 3.0 mm from the OD of the temporal retina; the peak density (12,857±353, mean±SD; n=3) appeared 0.3 mm from the OD in the nasal retina. The density gradient from the point of the highest density to the point of the lowest den-

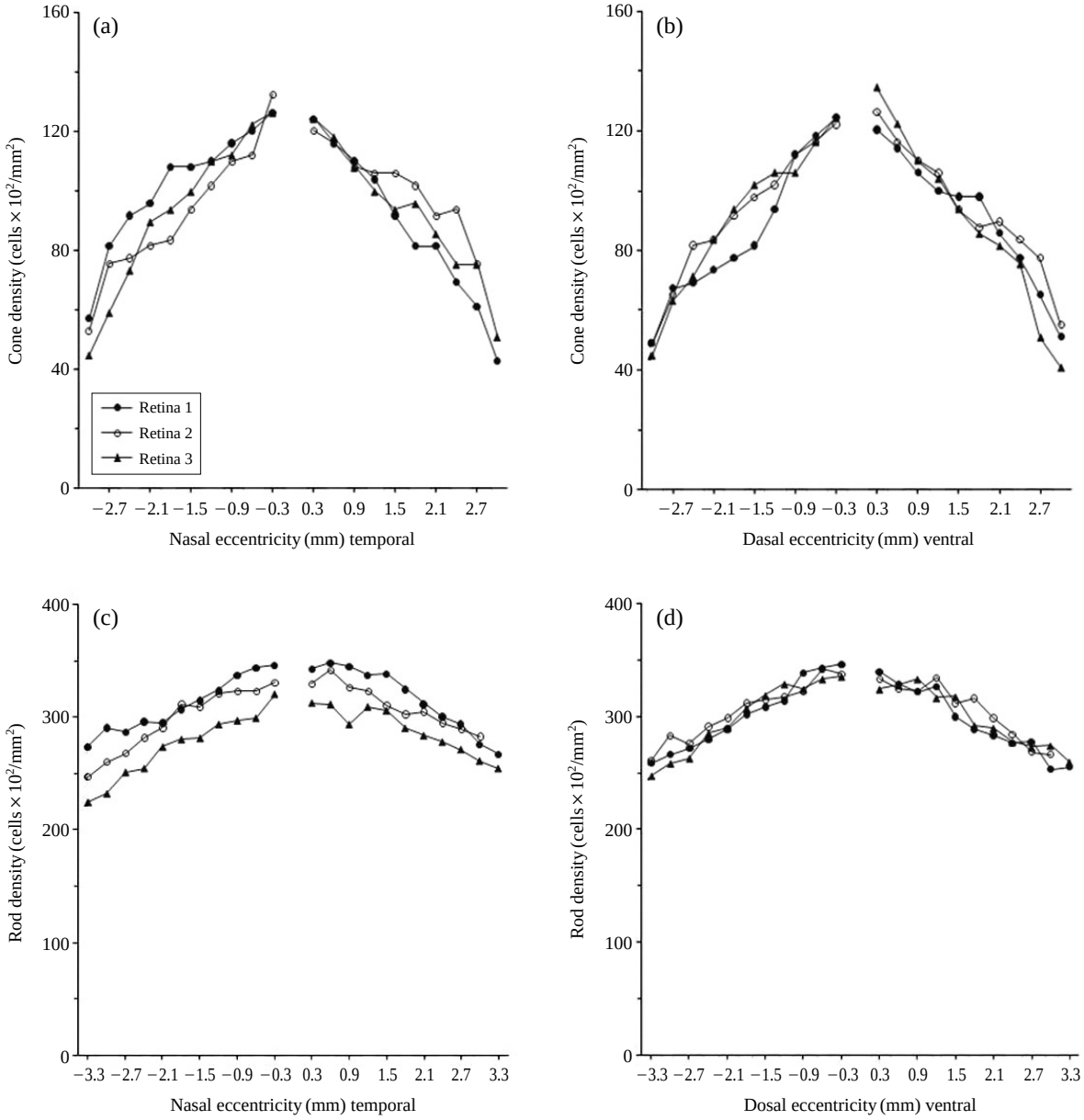

Fig. 2. Spatial densities of cones (a, b) and rods (c, d) encountered along two axes, nasotemporal (a, c) and dorsoventral (b, d), intersecting the optic nerve head.

sity was 2.74.

In three DAB-reacted whole mount retinas, rod cells in the photoreceptor cell layer were also counted. The estimated total number of rod cells varied from 9,277,576 to 9,633,198 cells among the three sampled in this study. Table 1 and Fig. 2 show the results. There were 9,633,198 cells in retina #1L, 9,433,677 cells in retina #2L, and 9,277,576 cells in retina #3R; therefore, the average number of rod cells/retina was 9,448,150±178,252 (mean±SD; n=3). The mean density of rod cells was 300,082 ±8,838 cells/mm^2 in the three retinas (Table 1). The distribution of total rod cells is shown in Fig. 2 and Table 2. The two graphs (Fig. 2c and 2d) show the numbers of cells encountered along the nasotemporal (Fig. 2c) and dorsoventral (Fig. 2d) axes intersecting the OD. The lowest density of rod cells (248,148±24,478, mean±SD; n=3) was found 3.3 mm from the OD of the nasal retina; and the peak density (340,000± 5,879, mean±SD; n=3) appeared 0.3 mm from the OD in the dorsal retina in this study. Thus, on average, rods are 96.99% and cones are 3.01% of all the photoreceptors. The density of rod cells has a slightly flatter distribution than that of cones.

Table 2. Distribution of photoreceptor at different locations in three retinas of Syrian hamster

	Retinal eccentricity																				
	D11	D10	D9	D8	D7	D6	D5	D4	D3	D2	D1	V1	V2	V3	V4	V5	V6	V7	V8	V9	V10	V11
Cone photoreceptors																						
Retina 1																						
Number of cells		24	33	34	36	38	40	46	55	58	61	59	56	52	49	48	48	42	38	32	27	
Density (cells/mm^2)		4,898	6,735	6,939	7,347	7,755	8,165	9,388	11,224	11,837	12,449	12,041	11,429	10,612	10,000	9,796	9,796	8,571	7,755	6,531	5,510	
Retina 2																						
Number of cells		24	32	40	41	45	48	50	55	57	60	62	57	54	52	46	43	44	41	38	27	
Density (cells/mm^2)		4,898	6,531	8,163	8,367	9,184	9,796	10,204	11,224	11,633	12,245	12,653	11,633	11,020	10,612	9,388	8,776	8,980	8,367	7,755	5,510	
Retina 3																						
Number of cells		22	31	35	41	46	50	52	52	57	61	66	60	54	51	46	42	40	37	25	20	
Density (cells/mm^2)		4,490	6,327	7,143	8,367	9,388	10,204	10,612	10,612	11,633	12,449	13,469	12,245	11,020	10,408	9,388	8,571	8,163	7,551	5,102	4,082	
Rod Photoreceptor																						
Retina 1																						
Number of cells	233	240	245	252	260	272	278	283	305	309	312	306	296	290	294	270	260	255	249	250	228	230
Density (cells/mm^2)	258,889	266,667	272,222	280,000	288,889	302,222	308,889	314,444	338,889	343,333	346,667	340,000	328,889	322,222	326,667	300,000	288,889	283,333	276,667	277,778	253,333	255,556
Retina 2																						
Number of cells	235	255	249	262	269	281	284	286	290	308	304	300	292	290	301	281	285	269	256	242	240	
Density (cells/mm^2)	261,111	283,333	276,667	291,111	298,889	312,222	315,556	317,778	322,222	342,222	337,778	333,333	324,444	322,222	334,444	312,222	316,667	298,889	284,444	268,889	266,667	
Retina 3																						
Number of cells	223	233	237	257	261	277	287	296	292	300	302	292	295	300	285	286	263	261	250	246	247	234
Density (cells/mm^2)	247,778	258,889	263,333	285,556	290,000	307,778	318,889	328,889	324,444	333,333	335,556	324,444	327,778	333,333	316,667	317,778	292,222	290,000	277,778	273,333	274,444	260,000

	N11	N10	N9	N8	N7	N6	N5	N4	N3	N2	N1	T1	T2	T3	T4	T5	T6	T7	T8	T9	T10	T11
Cone photoreceptors																						
Retina 1																						
Number of cells		28	40	45	47	53	53	54	57	59	62	61	57	54	51	45	40	40	34	30	21	
Density (cells/mm^2)		5,714	8,163	9,184	9,592	10,816	10,816	11,020	11,633	12,041	12,653	12,449	11,633	11,020	10,408	9,184	8,163	8,163	6,939	6,122	4,286	
Retina 2																						
Number of cells		26	37	38	40	41	46	50	54	55	65	59	57	53	52	52	50	45	46	37		
Density (cells/mm^2)		5,306	7,551	7,755	8,163	8,367	9,388	10,204	11,020	11,224	13,265	12,041	11,633	10,816	10,612	10,612	10,204	9,184	9,388	7,551		
Retina 3																						
Number of cells		22	29	36	44	46	49	54	55	60	62	61	58	53	49	46	47	42	37	37	25	
Density (cells/mm^2)		4,490	5,918	7,347	8,980	9,388	10,000	11,020	11,224	12,245	12,653	12,449	11,837	10,816	10,000	9,388	9,592	8,571	7,551	7,551	5,102	
Rod photoreceptors																						
Retina 1																						
Number of cells	246	261	258	266	265	276	283	291	303	309	311	308	313	310	303	304	292	280	270	264	248	240
Density (cells/mm^2)	273,333	290,000	286,667	295,556	294,444	306,667	314,444	323,333	336,667	343,333	345,556	342,222	347,778	344,444	336,667	337,778	324,444	311,111	30,000	393,333	275,556	266,667
Retina 2																						
Number of cells	222	234	241	253	261	280	278	288	290	290	297	296	307	293	290	279	272	274	265	260	254	
Density (cells/mm^2)	246,667	260,000	267,778	281,111	290,000	311,111	308,889	320,000	322,222	322,222	330,000	328,889	341,111	325,556	322,222	310,000	302,222	304,444	294,444	288,889	282,222	
Retina 3																						
Number of cells	202	209	226	229	246	252	253	264	267	269	288	281	280	264	278	275	261	255	250	244	235	229
Density (cells/mm^2)	224,444	232,222	251,111	254,444	273,333	280,000	281,111	293,333	296,667	298,889	320,000	312,222	312,222	311,111	293,333	308,889	290,000	283,333	277,778	271,111	261,111	254,444

D, dorsal; V, ventral; N, nasal; T, temporal

Table 3. Ratio of rod to cone densities encountered along two axes intersecting the optic nerve head of Syrian hamster

	Retinal eccentricity																				
	D10	D9	D8	D7	D6	D5	D4	D3	D2	D1	V1	V2	V3	V4	V5	V6	V7	V8	V9	V10
Retina 1L	54.44	40.42	40.35	39.32	38.97	37.83	33.49	30.19	29.01	27.85	28.24	28.78	30.36	32.67	30.62	29.49	33.06	35.68	42.53	45.98
Retina 2L	57.85	42.36	35.66	35.72	34.00	32.21	31.14	28.71	29.42	27.58	26.34	27.89	29.24	31.52	33.26	36.08	33.28	34.00	34.67	48.40
Retina 3R	57.66	41.62	39.98	34.66	32.78	31.25	30.99	30.57	28.65	26.95	24.09	26.77	30.25	30.43	33.85	34.09	35.53	36.79	53.57	67.23
Mean	56.65	41.47	38.66	36.57	35.25	33.76	31.88	29.82	29.03	27.46	26.22	27.81	29.95	31.54	32.58	33.22	33.96	35.49	43.59	53.87
SD	1.91	0.98	2.61	2.44	3.28	3.55	1.40	0.99	0.38	0.46	2.08	1.01	0.62	1.12	1.72	3.38	1.36	1.41	9.49	11.64

	Retinal eccentricity																			
	N10	N9	N8	N7	N6	N5	N4	N3	N2	N1	T1	T2	T3	T4	T5	T6	T7	T8	T9	T10
Retina 1L	30.70	28.35	29.07	29.34	28.94	28.51	27.31	27.49	29.90	31.26	32.35	36.78	39.75	38.11	4.32	50.75	35.12	32.18	64.25	64.29
Retina 2L	34.66	33.88	31.53	31.36	28.71	27.70	26.95	27.31	29.32	30.10	30.36	29.21	29.62	33.15	31.36	53.08	41.00	34.44	38.26	–
Retina 3R	30.44	29.83	28.11	26.62	26.43	24.41	25.29	25.08	26.38	28.76	29.33	32.90	30.23	33.06	36.79	51.72	42.43	34.63	35.90	51.18
Mean	31.93	30.68	29.57	29.11	28.03	26.87	26.52	26.63	28.53	30.04	30.68	32.96	33.20	34.77	24.16	51.85	39.52	33.75	46.14	57.74
SD	2.37	2.86	1.76	2.38	1.39	2.17	1.08	1.34	1.89	1.25	1.53	3.78	5.68	2.89	17.39	1.17	3.88	1.36	15.73	9.27

D, dorsal; V, ventral; N, nasal; T, temporal

The density gradient of rod cells from the point of the highest density to the point of the lowest density was 1.98. The density of cone and rod cells in hamster (Jeon et al., 1998) is similar to that of mouse in the present study.

The mean ratio of rod and cone in the hamster was 32.24 : 1. The ratios between rod and cone photoreceptors did not vary significantly with changes in eccentricity (Table 3). The lowest rod:cone ratio of 26.22 ± 2.08 (mean $\pm$ SD; n=3) : 1 was found in the central retina, 0.3 mm from the OD of the ventral retina. However, the ratio did not significantly increase in the peripheral retina. No areas showed three fold changes in the rod : cone ratio. The highest rod : cone ratio of 57.74 ± 9.27 (mean $\pm$ SD; n=3) : 1 was found in the far peripheral retina, 3.0 mm from the OD of the temporal retina.

In order to determine whether cones contain cone opsin, we labeled retina tissues with antibody against cone opsin, protein found in cone photoreceptors (Szél et al., 1996). Fig. 3 shows 50 μm vertical sections through a M/L- (Fig. 3a and 3b) and S- (Fig. 3c and 3d) cone opsin-immunoreactive hamster retina from a mid-pheripheral region. In the outer segment (arrowheads in Fig. 3b and 3d) of the outer nuclear layer, M/L- and S-cone opsin were found in many photoreceptors of the hamster retina.

DISCUSSION

As the knowledge about the spatial density and distribution of the photoreceptor is an indispensable part studying of the relationship between structure and function in retina, the number and distribution of cone and rod photoreceptors have been extensively studied in various animals such as human (Curcio et al., 1990), monkey (Packer et al., 1989; Wikler & Rakic, 1990; Wikler et al., 1990; Andrade et al., 2000), pig (Chandler et al., 1999), opossum (Kolb & Wang, 1985), cat (Steinberg et al., 1973; Hughes, 1975), rabbit (Hughes, 1971), rat (Hallett, 1987; Szél & Röhlich, 1992; Peichl, 2005), ground squirrel (Kryger et al., 1998), gerbil (Govardovskii et al., 1992), mouse (Jeon et al., 1998), salmonoid fish (Beaudet et al., 1997), mole (Glösmann et al., 2008), and bat (Kim et al., 2008). The retina is dominated by rod photoreceptors in most mammals. For example, human (Curcio et al., 1990) and rhesus monkey (Wikler et al., 1990) retinas contain approximately 95% of rod photoreceptors of all the photoreceptors. In most mammals, the range of rod density varies from almost 99% to approximately 85% (Govardovskii et al., 1992; Szél & Röhlich, 1992). How-

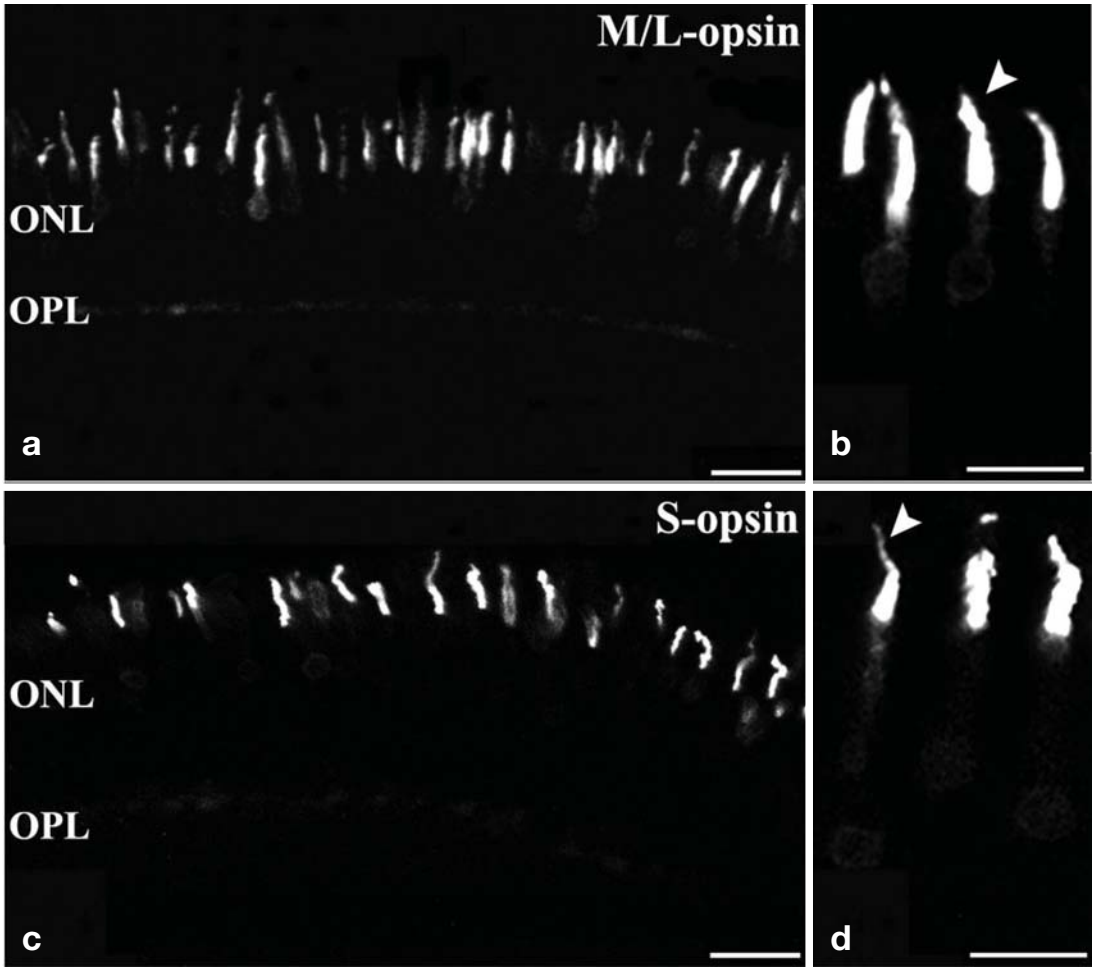

Fig. 3. Confocal micrographs of M/L-, S-opsin labeled cells in 50 μm vertical sections of fluorescence-reacted hamster retina. (a) M/L-opsin labeled cells were found in the ONL. (b) Higher magnification of M/L-opsin labeled photoreceptors in the ONL. (c) S-opsin labled cells were found in the ONL. (d) Higher magnification of S-opsin labeled photoreceptors in the ONL. Arrowheads in (b, d) indicate cone outer segment. M/L-opsin, middle-to-long-wave-sensitive-opsin; S-opsin, short-wave-sensitive-opsin; ONL, outer nuclear layer; OPL, outer plexiform layer. Scale bar=20 μm (a, c), Scale bar=30 μm (b, d).

ever, some mammalian retinas are dominated by cone photoreceptors. The tree shrew contains approximately 95% of cone photoreceptors of all the photoreceptors (Petry et al., 1993).

We have estimated the total number of rods and cones in three whole mounted hamster retinas using DIC optics in conjunction with peanut lectin labeling. In the present study, rods were 96.99%, and cones were 3.01% of all the photoreceptors. The population density of cone and rod cells in the present study is very similar to that of mouse. In mouse retina from our previous study (Jeon et al., 1998), we found that rods were 97.2%, and cones were 2.8% of all photoreceptors. Rat also contained 1～10% of cone photoreceptors of all the photoreceptors (Hallett, 1987; Szél & Röhlich, 1992; Peichl, 2005). Thus, the combined results indicate that the Rodentia rat, mouse and hamster show similar topographic properties of cone and rod photoreceptors. However, the Rodentia gerbil contained slightly higher numbers of cones: 13～14% of cone photoreceptor of all photoreceptors. By contrast, the Rodentia ground squirrel contained up to 95% of cones of all photoreceptors (Szél & Röhlich, 1988). These results indicate that the features and qualities of the visual processing are very different among the order Rodentia. As the differential constituents of cone and rod photoreceptors reflect diurnal and nocturnal behavior, respectively (Wikler and Rakic, 1990; Umino et al., 2008), the distribution of photoreceptor subtypes in the retina of hamster indicates that this is a nocturnal animal. It is also very interesting the population density of cone and rod cells in hamster retina is very similar to that of the nocturnal bat. In a Microchiroptera bat retina from our previous study (Kim et al., 2008), we found that rods were 97.5%, and cones were

2.5% of all photoreceptors.

In primate retina, both populations of photoreceptors have an area of high peak density: the fovea for the cones, and an area near the fovea for the rods. Thus, both cone and rod photoreceptor populations have a marked center-to-periphery gradient in photoreceptor density (Petry et al., 1993). However, hamster retina did not show a pronounced center-to-periphery gradient in photoreceptor density. The density gradient was 2.74 for cones and 1.98 for rods in the hamster retina. As expected, this is because of the lack of the fovea in rodents. The density gradient in hamster retina is slightly higher than that of mouse (Jeon et al., 1998). The data suggest the quality of visual acuity in central : peripheral areas in hamster retina is slightly lower than that of mouse. The average cone density in the hamster retina is similar found in the primate's retina at 3∼4 mm eccentricity (Packer et al., 1989). However, at the same eccentricity, the rod cell population is much higher in hamster retina than in the primate retina. These results indicate that one of the major differences in the photoreceptor mosaics between primate and the hamster is the higher density of the rod photoreceptors in the rodent.

In addition, the present study shows that hamster retina contains M/L-, S-opsins in cone photoreceptors. Cone opsins are related with color vision and can be further seperated into three subgroups, which are in accord well with their absorption spectra: L-opsins (red opsin), M-opsins (green opsin) and S-opsins (blue opsin). Thus, the existence of significant numbers of cone cells and the existence of M/L- and S-cone opsins in the present study strongly reflect visual abilities such as scotopic or color vision, resolution and detection acuity, spatial discrimination, and pattern recognition (Hirsch & Miller, 1987; Thibos et al., 1987; Williams & Coletta, 1987).

In conclusion, the hamster retina contains well-organized spatial density distribution and spatial density of cones and rods. Hamsters are strongly rod-dominated animals. Since the topographic property of these photoreceptors and the existence of M/L-, S-opsins in the cone photoreceptors has been considered to be one of the diverse factors in determining the features and quality of the vision, the present results should be importantly applicable to a better understanding of the visual processing in hamster visual system.

ACKNOWLEDGEMENTS

We thank Peter Durrant for proofreading the paper.

REFERENCES

Andrade da Costa BL, Hokoç JN: Photoreceptor topography of the retina in the New World monkey *Cebus apella*. Vision Res 40 : 2395-2240, 2000.

Beaudet L, Novales Flamarique I, Hawryshyn CW: Cone photoreceptor topography in the retina of sexually mature Pacific salmonid fishes. J Comp Neurol 383 : 49-59, 1997.

Blanks JC, Johnson LV: Specific binding of peanut lectin to a class of retinal photoreceptor cells. A species comparison. Invest Ophthalmol Vis Sci 25 : 546-557, 1984.

Bridges CD: Lectin receptors of rods and cones. Visualization by fluorescent label. Invest Ophthalmol Vis Sci 20 : 8-16, 1981.

Chandler MJ, Smith PJ, Samuelson DA, Mackay EO: Photoreceptor density of the domestic pig retina. Vet Ophthalmol 2 : 179-184, 1999.

Curcio CA, Sloan JKR, Packer O, Hendrickson AE, Kalina RE: Distribution of cones in human and monkey retina: Individual variability and radial asymmetry. Science 236 : 579-582, 1987.

Curcio CA, Sloan JKR, Kalina RE, Hendrickson AE: Human photoreceptor topography. J Comp Neurol 292 : 497-523, 1990.

Glösmann M, Steiner M, Peichl L, Ahnelt PK: Cone photoreceptors and potential UV vision in a subterranean insectivore, the European mole. J Vis 8 : 1-12, 2008.

Govardovskii VI, Röhlich P, Szél A, Khoklova TV: Cones in the retina of the Mongolian gerbil, *Meriones unguiculatus*; an immunocytochemical and electrophysiological study. Vision Res 32 : 19-27, 1992.

Hallett PE: The scale of the visual pathways of mouse and rat. Biol Cybern 57 : 275-286, 1987.

Hirsch J, Miller WH: Does cone positional disorder limit resolution? J Opt Soc Am A 4 : 1481-1492, 1987.

Hughes A: Topographical relationships between the anatomy and physiology of the rabbit visual system. Doc Ophthalmol 30 : 33-159, 1971.

Hughes A: A quantitative analysis of the cat retinal ganglion cell topography. J Comp Neurol 163 : 107-128, 1975.

Jeon CJ, Strettoi E, Masland RH: The major cell populations of the mouse retina. J Neurosci 18 : 8936-8946, 1998.

Jeon MH, Jeon CJ: Immunocytochemical localization of calretinin containing neurons on retina from rabbit, cat, and dog. Neurosci Res 32 : 75-84, 1998.

Kim TJ, Jeon YK, Lee JY, Lee ES, Jeon CJ: The photoreceptor populations in the retina of the greater horseshoe bat *Rhinolophus ferrumequinum*. Mol Cells 26 : 373-379, 2008.

Kolb H, Wang HH: The distribution of photoreceptor, dopaminergic amacrine cells and ganglion cells in the retina of the North American opossum (*Didelphis virginiana*). Vis Res 25 : 1207-1221, 1985.

Kryger Z, Galli-Resta L, Jacobs GH, Reese BE: The topography of rod and cone photoreceptors in the retina of the ground squirrel.

Vis Neurosci 15 : 685-691, 1998.
Packer O, Hendrickson AE, Curcio CA: Photoreceptor topography of the retina in the adult pigtail macaque (*Macaca nemestrina*). J Comp Neurol 288 : 165-183, 1989.
Packer O, Hendrickson AE, Curcio CA: Development redistribution of photoreceptors across the *Macaca nemestrina* (pigtail macaque) retina. J Comp Neurol 298 : 472-493, 1990.
Peichl L: Diversity of mammalian photoreceptor properties: adaptations to habitat and lifestyle? Anat Rec A Dicov Mol Cell Evol Biol 287 : 1001-1012, 2005.
Petry HM, Erichsen JT, Szél A: Immunocytochemical identification of photoreceptor populations in the tree shrew retina. Brain Res 616 : 344-350, 1993.
Rodieck RW: The First Steps in Seeing. Sinauer Associates, Sunderland, pp. 37-55, 1998.
Steinberg RH, Reid M, Lacy PL: The distribution of rods and cones in the retina of the cat (*Felis domesticus*). J Comp Neurol 148 : 229-248, 1973.
Szél A, Röhlich P: Four photoreceptor types in the ground squirrel retina as evidenced by immunocytochemistry. Vision Res 28 : 1297-1302, 1988.
Szél A, Röhlich P: Two cone types of rat retina detected by antivisual pigment antibody. Exp Eye Res 55 : 47-52, 1992.
Szél A, Röhlich P, Caffé AR, van Veen T: Distribution of cone photoreceptors in the mammalian retina. Microsc Res Tech 35 : 445-462, 1996.
Thibos LN, Walsh DJ, Cheney FE: Vision beyond the resolution limit: aliasing in the periphery. Vision Res 27 : 2193-2197, 1987.
Umino Y, Solessio E, Barlow RB: Speed, spatial, and temporal tuning of rod and cone vision in mouse. J Neurosci 28 : 189-198, 2008.
Wikler KC, Rakic P: Distribution of photoreceptor subtypes in the retina of diuranal and nocturnal primates. J Neurosci 10 : 3390-3401, 1990.
Wikler KC, Williams RW, Rakic P: Photoreceptor mosaic: number and distribution of rods and cones in the rhesus monkey retina. J Comp Neurol 297 : 499-508, 1990.
Williams DR, Colletta NJ: Cone spacing and the visual resolution limit. J Opt Soc Am A 4 : 1514-1523, 1987.

＜국문초록＞

본 연구에서는 햄스터 망막의 추상과 간상 광수용체의 양적 분석을 하였다. 추상 광수용체를 과산화 효소로 표지된 피넛 렉틴(peroxidase-labeled peanut lectin)을 사용하여 염색한 뒤 광학 미분간섭 현미경(DIC, differential interference contrast optics)을 사용하여 관찰하였다. 또한 면역세포화학적 방법으로 추상 광수용체에 위치한 M/L-옵신과 S-옵신을 염색한 뒤 공초점 형광 현미경(confocal microscope)을 사용하여 관찰하였다. 추상세포의 평균 밀도는 9,307 cells/mm^{2}이며 전체 추상세포는 293,060개였다. 추상세포의 최대값(12,857 cells/mm^2)은 맹점(시신경 유두, optic disk)로부터 코 쪽 망막(nasal retina)으로 0.3 mm 떨어진 곳에 위치하였다. 간상세포의 평균은 300,082 cells/mm^{2}으로 전체 간상세포는 9,448,150개였다. 간상세포의 최대값(340,000 cells/mm^2)은 맹점으로부터 등쪽 망막(dorsal retina) 방향으로 0.3 mm 떨어진 곳에서 발견되었다. 평균적으로 전체 광수용체 중, 간상세포의 전체 분포는 96.99%이고 추상세포는 3.01%를 차지하였다. 또한 간상과 추상의 평균 비는 32.24 : 1이었다. 햄스터의 추상세포는 M/L-와 S-옵신을 가진다. 본 연구 결과는 햄스터가 일부 명소시를 가지는 강한 간상 우세 망막임을 제시한다.